



Technical Report AC-TR-21-006

August 2021

A General Cooperative Optimization Approach for Distributing Service Points in Mobility Applications

Thomas Jatschka, Tobias Rodemann, and
Günther R. Raidl



This is the authors' copy of a paper that appeared in *MDPI Algorithms* 14, 8, Article 232 (August 2021). DOI:

www.ac.tuwien.ac.at/tr

A General Cooperative Optimization Approach for Distributing Service Points in Mobility Applications

Thomas Jatschka ^{1*}, Günther R. Raidl ¹ and Tobias Rodemann ²

¹ Institute of Logic and Computation, TU Wien, Austria; {tjatschk|raidl}@ac.tuwien.ac.at

² Honda Research Institute Europe, Germany; tobias.rodemann@honda-ri.de

* Correspondence: tjatschk@ac.tuwien.ac.at

Abstract: This article presents a cooperative optimization approach (COA) for distributing service points for mobility applications, which generalizes and refines a previously proposed method. COA is an iterative framework for optimizing service point locations, combining an optimization component with user interaction on a large scale and a machine learning component that learns user needs and provides the objective function for the optimization. The previously proposed COA was designed for mobility applications in which single service points are sufficient for satisfying individual user demand. This framework is generalized here for applications in which the satisfaction of demand relies on the existence of two or more suitably located service stations, such as in the case of bike/car sharing systems. A new matrix factorization model is used as surrogate objective function for the optimization, allowing to learn and exploit similar preferences among users w.r.t. service point locations. Based on this surrogate objective function, a mixed integer linear program is solved to generate an optimized solution to the problem w.r.t. the currently known user information. User interaction, refinement of the matrix factorization, and optimization are iterated. An experimental evaluation analyzes the performance of COA with special consideration of the number of user interactions required to find near optimal solutions. The algorithm is tested on artificial instances as well as instances derived from real-world taxi data from Manhattan. Results show that the approach can effectively solve instances with hundreds of potential service point locations and thousands of users while keeping the user interactions reasonably low. A bound on the number of user interactions required to obtain full knowledge of user preferences is derived, and results show that with 50% of performed user interactions the solutions generated by COA feature optimality gaps of only 1.45% on average.

Keywords: Heuristic optimization; Location planning; Cooperative optimization; Preference learning

Citation: Jatschka, T.; Raidl, G.; Rodemann, T. A General Cooperative Optimization Approach for Distributing Service Points in Mobility Applications. *Algorithms* **2021**, *1*, 0. <https://doi.org/>

Received:

Accepted:

Published:

Publisher's Note: MDPI stays neutral with regard to jurisdictional claims in published maps and institutional affiliations.

Copyright: © 2021 by the authors. Submitted to *Algorithms* for possible open access publication under the terms and conditions of the Creative Commons Attribution (CC BY) license (<https://creativecommons.org/licenses/by/4.0/>).

1. Introduction

A fundamental ingredient for optimizing the locations of service points in mobility applications, such as charging stations for electric vehicles or pickup and drop-off stations for car/bike sharing systems, is the distribution of existing customer demand to be potentially fulfilled in the considered geographical area. While there exists a vast amount of literature regarding setting up service points for mobility applications, such as vehicle sharing systems ([1–4]) or charging stations for electric vehicles [5–8], estimations of the existing demand distribution are usually obtained upfront by performing customer surveys, considering demographic data, information on the street network and public transport, and not that seldom including human intuition and political motives. However, such estimations are frequently imprecise and a system built on such assumptions might not perform as effectively as it was originally hoped for. For example in [9] GPS-based travel survey data of fossil fueled cars is used for setting up charging stations for electric vehicles. However, as pointed out by Pagany et al. [10], it cannot be assumed that the driving behavior of customers remains unchanged when

39 switching from fossil fueled cars to electric vehicles. Furthermore, Pagany et al. [10]
40 present a survey of 119 publications for locating charging stations for electric vehicles in
41 which they also discuss further problems with the above mentioned demand estimation
42 methods.

43 A more frequent usage of a service system by a customer will in general depend
44 not only on the construction of a single service point on a particular location but more
45 globally on non-trivial relationships of the customer's necessities and preferences in
46 conjunction with larger parts of the whole service system. For example in the case of
47 bike/car sharing systems, a well placed rental station close to the origin of a trip might be
48 worthless if there does not also exist a suitable location near the destination for returning
49 the vehicle. Furthermore, some customers might use multiple modes of transport for
50 a single trip [11]. Consequently, some more distant service station for returning the
51 vehicle might be acceptable if this place is well connected by public transport used for an
52 additional last leg [12]. Thus, there also might be alternatives for fulfilling demand that
53 cannot all be exactly specified by potential users. The example with an additional leg by
54 public transport also illustrates that geographical closeness is not always the deciding
55 factor.

56 To address these issues Jatschka et al. [13] proposed the concept of a *Cooperative*
57 *Optimization Algorithm* (COA) which, instead of estimating customer demand upfront,
58 directly incorporates potential users in the location optimization process by iteratively
59 confronting them with location scenarios and asking for evaluation. Based on the
60 user feedback a machine learning model is trained which is then used as surrogate
61 objective function to evaluate solutions in an optimization component. User interaction,
62 a corresponding refinement of the surrogate objective function, and the optimization
63 are iterated. Expected benefits of such a cooperative approach are a faster and easier
64 data acquisition [14], the direct integration of users into the whole location planning
65 process, a possibly stronger emotional link of the users to the product, and ultimately
66 better understood [15] and more accepted optimization results [14]. Potential customers
67 further know local conditions and their particular properties, including also special
68 aspects that are not all easily foreseen in a classical demand acquisition approach. To
69 the best of our knowledge such an approach has not yet been considered in the area of
70 locating service points for mobility applications.

71 As the initial proof-of-concept approach in [13] did not scale well to larger appli-
72 cation scenarios, we described a more advanced cooperative optimization approach
73 relying on matrix factorization in a preliminary conference paper [16]. The current article
74 deepens and extends this work in particular in the following aspects.

75 We now apply a more advanced matrix factorization originally introduced in [17],
76 which allows to exploit that only a small fraction of locations is actually relevant for each
77 user and that user data is not missing at random.

78 Moreover, the COA in [16] considered only mobility applications in which single
79 service points are sufficient for satisfying a particular demand of a user, such as the
80 placement of charging stations for electric vehicles. The main contribution of this paper
81 is to extend the solution approach towards applications in which the satisfaction of
82 demand typically relies on the existence of suitable pairs or more generally tuples of
83 service stations, such as in the case of bike or car sharing systems where a vehicle is first
84 picked up at a rental station near the origin and returned at a station within easy reach
85 of the destination.

86 This extended framework is tested on different artificial benchmark scenarios using
87 an idealized simulation of user interactions. The benchmark scenarios were hereby
88 created in a controlled way so that optimal reference solutions could be obtained for
89 comparison. One group of benchmark scenarios was derived from real world taxi trip
90 data from Manhattan. To characterize the amount of user interaction COA requires, an
91 upper bound on the number of necessary non-redundant user interactions for obtaining
92 full knowledge of user preferences is derived as baseline. Results on our instances show

93 that solutions generated by COA feature optimality gaps of only 1.45% on average with
94 50% of performed user interactions.

95 The next Section discusses related work. In Section 3 we introduce our formal
96 problem setting, the *Generalized Service Point Distribution Problem (GSPDP)*, which reflects
97 the essence of various location problems for mobility services. Afterwards, in Section
98 4, we detail the cooperative optimization framework for solving the GSPDP. Section
99 5 describes how benchmark scenarios for testing were generated, and in Section 6 we
100 present and discuss experimental results. Section 7 concludes this work with an outlook
101 on promising future work.

102 2. Related Work

103 The considered problem in general falls into the broad category of facility location
104 problems, i.e., optimization problems where facilities should be set up on a subset of
105 given potential locations as economically as possible in order to fulfill a certain level of
106 customer demand. Similarly to a p-median or maximal covering location model, see
107 [18], we limit the facilities to be opened. However, instead of imposing a direct limit on
108 the number of facilities, in our formulation a maximum budget for setting up facilities
109 is specified and each facility is associated with setup costs. In general our problem can
110 be classified as an uncapacitated fixed charge Facility Location Problem (FLP), see [19],
111 however, without explicitly given demands (see below). Moreover, our problem also
112 has similarities to stochastic or robust FLPs [20] in which problem inputs, such as the
113 demand, may be uncertain. For such problems uncertain inputs are usually modeled via
114 random variables [21] or scenario-based approaches [22]. For a survey on FLPs see [23].

115 In our problem formulation we have mobility applications in mind, such as the
116 distribution of charging stations for electric vehicles or setting up rental stations for
117 car/bike sharing. While there already exists a vast amount of literature for setting up
118 such systems to the best of our knowledge all existing work essentially assumes customer
119 demand to be estimated upfront. For example, [24] and [8] use parking information to
120 identify promising locations for electric vehicle charging stations. [25] locate charging
121 stations for an on-demand bus system using taxi probe data of Tokyo. Moreover, census
122 data are commonly used for estimating demand for car sharing systems [26], bike sharing
123 systems [27], or for setting up electric vehicle charging stations [28]. Data mining and
124 other related techniques are also often employed to detect traffic patterns for bike sharing
125 systems [29,30] as well as car sharing systems [31].

126 Ciari et al. [32] recognize the difficulties in making demand predictions for new
127 transport options based on estimated data and therefore propose to use an activity-based
128 microsimulation technique for the modeling of car sharing demand. The simulation is
129 done with help of the travel demand simulator MATSim [33].

130 There also exist some works that take user preferences into account, e.g., in [34] a
131 car sharing system is designed based on different assumptions on the behavior of users.
132 The authors come to the conclusion that providing real-time information to customers
133 can greatly improve the service level of a system if users are willing to visit a different
134 station if their preferred one does not have a vehicle available.

135 In our approach we substantially deviate from this traditional way of acquiring
136 existing demand upfront and instead resort to an interactive approach. Potential future
137 customers are directly incorporated in the optimization process as an integral part by
138 iteratively providing feedback on meaningfully constructed location scenarios. In this
139 way we learn user demands on-the-fly and may avoid errors due to unreliable a priori
140 estimations. For a survey on interactive optimization algorithms in general see [14].
141 The performance of interactive algorithms is strongly influenced by the quality of the
142 feedback given by the interactors. Too many interactions with a user will eventually
143 result in user exhaustion [35], negatively influencing the reliability of the obtained
144 feedback. Additionally, interacting with users can be quite time consuming, even when
145 dealing with a single user. Hence, in order to keep the interactions with users low one

146 can resort to surrogate-based optimization approaches [36,37]. Surrogate models are
 147 typically machine learning models serving as proxy of functions that are difficult to
 148 evaluate [38]. In [16] as well as in this contribution we make use of a matrix factorization
 149 [39] based surrogate model. Matrix factorization is a collaborative filtering technique
 150 which is frequently used in recommender systems, see e.g., [40].

151 As already pointed out, the basic concept of COA was already presented in [13],
 152 where we made use of an adaptive surrogate model [41]. The underlying structure
 153 of this surrogate model is formed by a large set of individual smaller models, i.e.,
 154 one machine learning model for each combination of user and potential service point
 155 location, which are trained with the feedback of the respective users. While initially
 156 being instantiated by simple linear models, these machine learning models are step-wise
 157 upgraded as needed to more complex regressors during the course of the algorithm in
 158 order to cope with possibly encountered higher complexity. Specifically in [13], each
 159 linear model can be upgraded to a neural network. The number of neurons in the hidden
 160 layer is increased whenever the training error exceeds a certain threshold. Overfitting
 161 is effectively avoided by making the individual models not unnecessarily large. A
 162 Variable Neighborhood Search (VNS) [42] was used as optimization core to generate
 163 new solutions w.r.t. the current surrogate function. In [43] the performance of the VNS
 164 optimization core was compared to an optimization core using a population-based
 165 iterated greedy approach [44]. Unfortunately, this first realization of COA exhibits severe
 166 limitations in the scalability to larger numbers of potential service point locations and/or
 167 users, in particular as all users are considered independently of each other.

168 The current work builds upon the observation that in a larger user base there are
 169 typically users sharing the same or similar needs or preferences. Identifying these shared
 170 demands and exploiting them to improve scalability as well as to reduce the required
 171 feedback per user is a main goal here. While the basic principles of COA remain the
 172 same, major changes are performed in the way the approach interacts with users, how
 173 the feedback of users is processed, as well as how new candidate solutions are generated.
 174 Moreover, the adaptive surrogate model from [13] realized by the large set of underlying
 175 simpler machine learning models is replaced by a single matrix factorization based
 176 model that is able to exploit said similarities between users. Besides our aforementioned
 177 preliminary conference paper already sketching the application of a matrix factorization
 178 within COA [16], to the best of our knowledge there exists no further work on interactive
 179 optimization approaches for location planning in mobility applications.

180 3. The Generalized Service Point Distribution Problem

181 The *Generalized Service Point Distribution Problem* (GSPDP) considered here is an
 182 extension of the *Service Point Distribution Problem* (SPDP) introduced in [16]. Given
 183 are a set of locations $V = \{1, \dots, n\}$ at which service points may be set up and a set
 184 of potential users $U = \{1, \dots, m\}$. The fixed costs for establishing a service point at
 185 location $v \in V$ are $z_v^{\text{fix}} \geq 0$, and this service point's maintenance over a defined time
 186 period is supposed to induce variable costs $z_v^{\text{var}} \geq 0$. The total setup costs of all stations
 187 must not exceed a maximum budget $B > 0$. Furthermore, it is assumed that opened
 188 service stations are able to satisfy an arbitrary amount of customer demand. For each
 189 unit of satisfied customer demand a prize $q > 0$ is earned.

A solution to the GSPDP is a subset $X \subseteq V$ of all locations where service points are
 to be set up. A solution X is feasible if its total fixed costs do not exceed the maximum
 budget B , i.e.,

$$z^{\text{fix}}(X) = \sum_{v \in X} z_v^{\text{fix}} \leq B. \quad (1)$$

190 Given the set of users U , we assume that each user $u \in U$ has a certain set of *use*
 191 *cases* C_u , such as going to work, to a recreational facility, or shopping. Each use case
 192 $c \in C_u$ is associated with a demand $D_{u,c} > 0$ expressing how often the use case is
 193 expected to be frequented by user u within some defined time period such as a week

194 or a month. For each unit of satisfied customer demand a prize $q > 0$ is earned. The
 195 demand of each use case can possibly be satisfied by different service points or subsets
 196 of service points to different degrees, depending on the concrete application and the
 197 customer's preferences. Note that use cases are here just labels and are not directly
 198 associated with specific geographic locations. This separation is intentionally done in
 199 order to keep flexibility: some use cases like shopping or the visit of a fitness center may
 200 possibly be realized at different places, and as already mentioned occasionally a service
 201 station farther away from a specific target location may also be convenient if some other
 202 mode of transportation is used as additional leg.

203 Depending on the actual application and characteristics of a use case, demand may
 204 be fulfilled by a single service station, e.g., when charging batteries of an electric vehicle,
 205 or a suitable combination of multiple service stations may be needed, such as when
 206 renting a vehicle at one place and returning it somewhere else. While [16] just considered
 207 the first case, we pursue here the general case of possibly requiring multiple service
 208 points to fulfill demand for a single use case.

209 To model this aspect formally, we associate each use case c of a user u with a set
 210 of *Service Point Requirements* (SPR) $R_{u,c}$. Similar to use cases these SPRs are not directly
 211 associated with geographic locations but are an abstract entity like "place within easy
 212 reach of home to rent a vehicle" or "place close to a supermarket to return a vehicle" with
 213 which a user can express the dependency on multiple service points to fulfill the needs
 214 of one use case. Thus, the demand of such a use case can only be satisfied if a service
 215 point exists at a suitable location for each of the use case's SPRs. Note that multiple use
 216 cases of a user may also share the same SPR(s). For example a use case referring to a trip
 217 from home to work and one from home to a supermarket may share the SPRs "place
 218 within easy reach of home to rent a vehicle". The set of all different SPRs over all use
 219 cases of a user u is denoted by $R_u = \bigcup_{c \in C_u} R_{u,c}$. Moreover, let $R = \bigcup_{u \in U} R_u$ be the set of
 220 all SPRs over all users. Note that in this notation, different users never share the same
 221 SPR labels, although labels may refer to similar SPRs.

222 For indicating how suitable a location is w.r.t. to an SPR we define values $w_{r,v} \in [0, 1]$
 223 indicating the suitability of a service point at location $v \in V$ to satisfy the needs of user
 224 $u \in U$ concerning SPR $r \in R_{u,c}$ in the use case $c \in C_u$. A value of $w_{r,v} = 1$ represents
 225 perfect suitability while a value of zero means that location v is unsuitable; values in
 226 between indicate partial suitability.

With these suitability values in mind, the objective of the GSPDP is to maximize

$$f(X) = q \cdot \sum_{u \in U} \sum_{c \in C_u} D_{u,c} \cdot \min_{r \in R_{u,c}} \left(\max_{v \in X} w_{r,v} \right) - \sum_{v \in X} z_v^{\text{var}}. \quad (2)$$

227 In the first term of this objective function, the obtained prize for the expected total
 228 satisfied demand is determined by considering for each user u , each use case c , and each
 229 SPR r a most suitable location $v \in V$ at which a service point is to be opened ($v \in X$).
 230 Over all SPRs of a use case, the minimum of the obtained suitability values is taken
 231 so that the full demand is only fulfilled when for each SPR an ideally suited service
 232 station is planned, and no demand is fulfilled as soon as one of the SPRs does not have
 233 an appropriate service point. The second term of the objective function represents the
 234 total maintenance costs for the service stations.

By linearizing the above objective function, the GSPDP can be formulated as a mixed
 integer linear program (MILP) with the following variables. Binary variables x_v indicate
 whether or not a service point is deployed at location $v \in V$, i.e., the binary vector
 $x = (x_v)_{v \in V}$ is the incidence vector of a corresponding solution $X \subset V$. Additional
 variables $h_{r,v}$ are used to indicate the actually used location $v \in V$ for each SPR $r \in R$.

The degree to which a use case $c \in C_u$ of a user $u \in U$ can be satisfied is expressed by continuous variables $y_{u,c} \in [0, 1]$. The GSPDP is then stated as follows.

$$\max \quad q \cdot \sum_{u \in U} \sum_{c \in C_u} D_{u,c} y_{u,c} - \sum_{v \in V} z_v^{\text{var}} x_v \quad (3)$$

$$\sum_{v \in V} z_v^{\text{fix}} x_v \leq B \quad (4)$$

$$\sum_{v \in V} h_{r,v} \leq 1 \quad \forall r \in R \quad (5)$$

$$\sum_{v \in V} w_{r,v} \cdot h_{r,v} \geq y_{u,c} \quad \forall u \in U, c \in C_u, r \in R_{u,c} \quad (6)$$

$$h_{r,v} \leq x_v \quad \forall v \in V, r \in R \quad (7)$$

$$x_v \in \{0, 1\} \quad \forall v \in V \quad (8)$$

$$0 \leq y_{u,c} \leq 1 \quad \forall u \in U, c \in C_u \quad (9)$$

$$0 \leq h_{r,v} \leq 1 \quad \forall r \in R, v \in V \quad (10)$$

235 In correspondence to the definition of f , the objective value is calculated in (3) as the sum
 236 of the prizes earned for fulfilled demand minus the costs for opening service stations.
 237 Inequality (4) ensures that the budget is not exceeded. Inequalities (5) ensure that at
 238 most one location is selected for each SPR. As our objective is to maximize the revenue it
 239 is ensured that always a suitable service point location with the highest suitability value
 240 for each SPR is chosen. Inequalities (6) determine the degrees to which the use cases
 241 are satisfied, considering that the actually fulfilled demand of a use case is assumed to
 242 be proportional to the minimum suitability value of the locations selected for the SPRs
 243 of the use case. Last but not least, Inequalities (7) ensure that only locations at which
 244 service points are to be opened can be used for SPRs and, thus, to satisfy demand of use
 245 cases. The size of this model in terms of the number of variables as well as the number
 246 of constraints is in $\mathcal{O}(m n |R|)$.

247 **Theorem 1.** *The GSPDP is NP-hard.*

248 **Proof.** NP-hardness of the GSPDP is proven by providing a reduction from the well
 249 known NP-hard Maximal Covering Location Problem (MCLP) [45] in the variant stated
 250 by Farahani *et al.* [46]. Given are a set of possible facility locations \mathcal{J} , a maximum
 251 number p of facilities to be opened, and a set of demand nodes \mathcal{D} . Moreover, each
 252 demand node $i \in \mathcal{D}$ is associated with a demand $a_i \geq 0$ and a subset of facilities $\mathcal{F}_i \subseteq \mathcal{J}$
 253 of which each is able to cover the node's full demand. The goal of the MCLP is to select
 254 up to p locations for opening facilities in order to maximize the total demand covered.

255 Given an instance to the MCLP we construct a corresponding GSPDP instance in
 256 which the set of locations V corresponds to the set of facilities \mathcal{J} and the set of users
 257 U corresponds to the set of demand nodes \mathcal{D} . Moreover, each user $u \in U$ only has a
 258 single use case with a single SPR and demand a_i with $u = i$. Building costs z_v^{fix} for a
 259 location $v \in V$ are set to one while the maintenance costs z_v^{var} are zero. The budget of
 260 the GSPDP instance is set to p , and the prize for a unit of covered demand q is set to
 261 one. The suitability value $w_{r,v}$ is set to one for $v \in V$ and $r \in R$ if facility i can satisfy the
 262 demand of demand node j , i.e., $j \in \mathcal{F}_i$, and zero otherwise.

263 Let (x, y, h) be a feasible solution to this derived GSPDP instance. A corresponding
 264 feasible solution to the MCLP is obtained by opening facilities at all locations $j \in \mathcal{J}$ for
 265 which $x_v = 1$. Due to the budget constraint (4), at most p facilities are opened in the
 266 MCLP instance, and thus, there is a bijective mapping of feasible GSPDP solutions to
 267 feasible MCLP solutions.

268 Since each user in the GSPDP instance only has one use case and each use case
 269 only consists of one SPR, the sets U , C , and R all contain the same elements. By our
 270 definitions, variables $y_{u,c}$ indicating the covered SPRs therefore also indicate the covered

271 demand nodes of the MCLP instance. More generally, we also have a bijective mapping
 272 of covered SPRs in the GSPDP instance to covered demand nodes in the MCLP instance.
 273 Last but not least, due to our definitions of the suitability values $w_{r,v}$, the fixed and
 274 variable costs for opened stations, and the prize per unit of fulfilled demand, the objective
 275 values of corresponding GSPDP and MCLP solutions also correspond. Since all applied
 276 transformations require polynomial time, it follows that the GSPDP is NP-hard. \square

277 In the next section we present a cooperative algorithm for solving the GSPDP when
 278 no a priori information about the suitability values $w_{r,v}$ of potential locations is known
 279 but can only be obtained by querying the users in a limited fashion.

280 4. The Cooperative Optimization Algorithm

281 A crucial aspect for solving the GSPDP is that determining the suitability values
 282 $w_{r,v}$ is no trivial task. While a user may be able to list a small number of best suited
 283 service station locations for each of his/her SPRs, we have to consider it practically
 284 infeasible to obtain reasonably precise suitability values for all potential service station
 285 locations V of each SPR by directly asking the users. A complete direct questioning
 286 would not only be extremely time consuming but users would easily be overwhelmed
 287 by the large number of possibilities, resulting in incorrect information. For example,
 288 users easily tend to only rate their preferred options as suitable and might not consider
 289 certain alternatives as also feasible although they actually might be on second thought
 290 when no other options are available. The problem of user fatigue substantially impacting
 291 the quality of obtained feedback when too much information is asked from a user is, for
 292 example, discussed in [35].

293 Hence, interaction with users needs to be kept to a minimum and should be done
 294 wisely to extract as much meaningful information as possible. Moreover, users must be
 295 confronted with easy questions whose answers at the same time provide strong guidance
 296 for the target system. Based on this philosophy, we present a *Cooperative Optimization*
 297 *Algorithm (COA)* for solving the GSPDP if no a priori information about the use cases
 298 of the users, their respective demands, or the suitability values is known. The general
 299 concept of COA was originally introduced in [13]. In this paper this framework is
 300 substantially adapted and extended towards better scalability and for solving instances
 301 of the more general GSPDP as specified in the previous section.

302 In Section 4.3 we formally define how users can interact with COA. Note however
 303 that COA does not put a strict limit on the number of allowed interactions with each
 304 user. Instead, we will measure the effectivity of our COA framework by the number of
 305 user interactions the framework requires for generating a (close to) optimal solution.

306 4.1. Methodology

307 In this subsection a high level overview of COA is given before detailing the
 308 individual components in successive subsections. Figure 1 shows the basic methodology:
 309 In each iteration the algorithm first generates location scenarios for a subset of users
 310 to evaluate. Based on the users' ratings of the scenarios, a surrogate objective function
 311 is continuously updated over the iterations. The GSPDP instance with the current
 312 surrogate objective function is then solved, yielding a solution. In the next iteration, this
 313 solution is a basis for deriving further meaningful location scenarios to be presented to
 314 users again. The surrogate objective function thus learns to represent the users' needs,
 315 more specifically the suitability values $w_{r,v}$, better and better, and the solutions obtained
 316 from the optimization will become more precise over time. Figure 2 exemplifies how the
 317 evaluation of a location scenario may look like from the perspective of a user.

318 From a technical point-of-view, the COA framework consists of a *Feedback Component*
 319 *(FC)*, an *Evaluation Component (EC)*, an *Optimization Component (OC)*, and a *Solution*
 320 *Management Component (SMC)*.

321 First, the FC is called starting an initialization phase by asking each user $u \in U$ to
 322 specify the user's use cases C_u , associated SPRs $R_{u,c}$, as well as corresponding demands

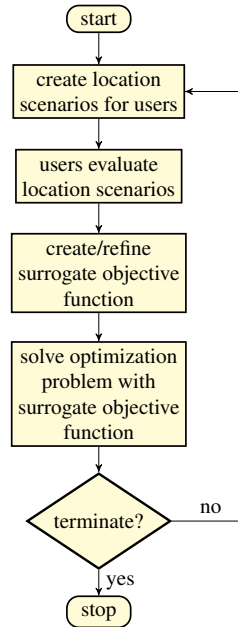


Figure 1. Basic methodology of the COA framework.

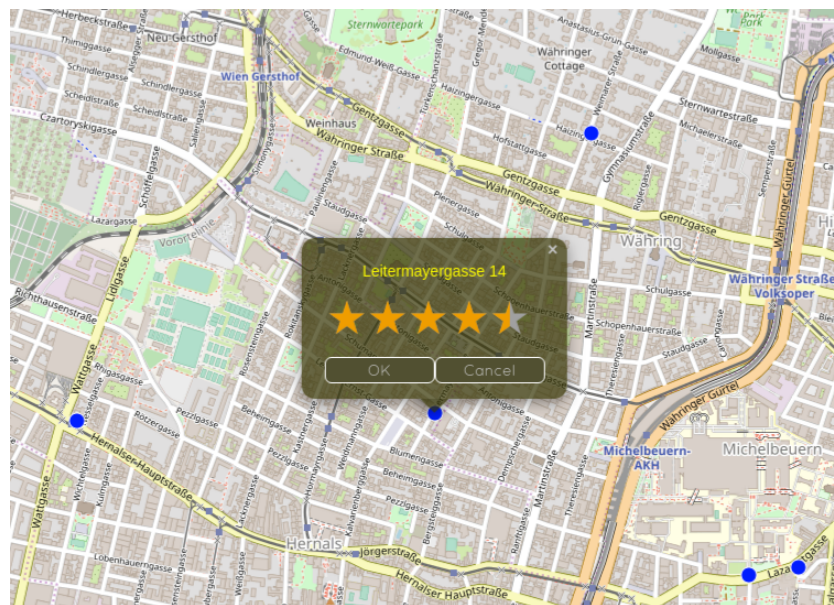


Figure 2. Exemplary evaluation of a location scenario by a user in the COA framework: A potential solution in form of a map with highlighted locations is presented, and the user can then provide suitability values for the highlighted locations in the form of ratings.

323 $D_{u,c}$, $c \in C_u$. Afterwards, the FC is responsible for collecting information from the
 324 user, i.e., users can interact with the framework at this stage of the algorithm. User
 325 information is collected by generating individual location scenarios for each user which
 326 are presented to the user in order to obtain his/her feedback. A user $u \in U$ then has to
 327 provide suitability values $w_{r,v}$ for locations $v \in S$ of solution scenarios S presented to
 328 him in respect to a use case requirement $r \in R_u$.

The feedback obtained from the users is processed in the EC. The EC maintains and continuously updates a *surrogate suitability function* $\tilde{w}_{\Theta}(r, v)$ approximating the suitability values $w_{r,v}$ of service point locations $v \in V$ w.r.t. SPR $r \in R$ without interacting with the respective user. This function is realized by a machine learning model with parameters

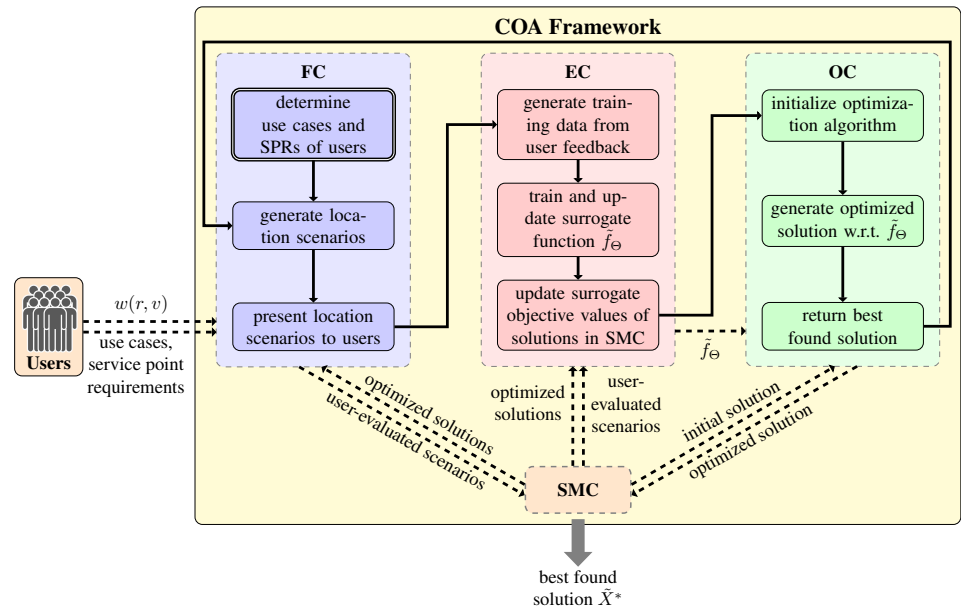


Figure 3. Components of COA and their interaction. The framework consists of the feedback component (FC), the evaluation component (EC), the optimization component (OC), and the solution management component (SMC). Users interact with the framework via the FC.

(weights) Θ . Based on this surrogate function, the EC also provides the surrogate objective function

$$\tilde{f}_{\Theta}(X) = q \cdot \sum_{u \in U} \sum_{c \in C_u} D_{u,c} \cdot \min_{r \in R_{u,c}} \left(\max_{v \in X} \tilde{w}_{\Theta}(r, v) \right) - \sum_{v \in X} z_v^{\text{var}} \quad (11)$$

329 with which a candidate solution X can be approximately evaluated. This fast approxi-
 330 mate evaluation is in particular important for intermediate candidate solutions generated
 331 during the optimization process which are not evaluated by the users. The respective
 332 learning mechanism of the surrogate objective function is also part of the EC.

333 A call of the OC is supposed to determine an optimal or close-to-optimal solution
 334 to the problem with respect to the EC's current surrogate objective function \tilde{f}_{Θ} . Note
 335 that the surrogate objective function never changes during a call of the OC, only in each
 336 major iteration of the framework after having obtained new user feedback. With the
 337 exception of the first call, the optimization procedure of the OC is warm-started with the
 338 current best solution \tilde{X}^* as initial solution to possibly speed up the optimization process.

339 Finally, the SMC efficiently stores and manages information on all candidate solu-
 340 tions that are relevant for more than one of the above components and in particular also
 341 the location scenario evaluations provided by the users so far as well as the solutions
 342 X_{OC} returned by the OC.

343 The whole process is repeated until some termination criterion is reached, e.g., the
 344 discrepancy of user feedback and the results of the EC is small enough or a maximum
 345 number of user interactions has been reached. In the end, COA returns a solution with
 346 the highest surrogate objective value of all of the so far generated solutions.

347 Figure 3 and Algorithm 1 give a summary of the whole COA procedure and of the
 348 main tasks of each of the components of COA.

349 In the next subsections we describe each component's functionality in more detail.

350 4.2. Solution Management Component

351 The SMC stores and manages so far considered solutions and evaluations by the
 352 users. The set of solutions obtained from the OC in all major iterations is stored in a set
 353 we denote by \mathcal{X} . For each solution $X \in \mathcal{X}$ the SMC keeps track of its current surrogate

Algorithm 1: Basic Framework

Input: an instance of the GSPDP
Output: best solution $\tilde{X}^* \subseteq V$ found

- 1: **Feedback Component:**
- 2: **for** $u \in U$ **do**
- 3: obtain use cases C_u with associated demands $D_{u,c}$ and service point requirements $R_{u,c}, \forall c \in C_u$, from user u ;
- 4: **end for**
- 5: **while** *no termination criterion satisfied* **do**
- 6: **Feedback Component:**
- 7: **for** *each scenario generation strategy* S_r **do**
- 8: $R' \leftarrow$ random sample of R ;
- 9: **for** $r \in R'$ **do**
- 10: $S_r \leftarrow$ generate set of location scenarios according to strategy S_r ;
- 11: present scenario to the corresponding user;
- 12: update SMC with ratings obtained from S_r ;
- 13: **end for**
- 14: **end for**
- 15: **Evaluation Component:**
- 16: train surrogate model \tilde{w}_Θ , yielding updated surrogate obj. function \tilde{f}_Θ ;
- 17: re-evaluate all solutions stored in the SMC with new \tilde{f}_Θ ;
- 18: **Optimization Component:**
- 19: $X_{OC} \leftarrow$ generate optimal solution w.r.t. the EC's \tilde{f}_Θ ;
- 20: update SMC with X_{OC} ;
- 21: **end while**
- 22: **return** *overall best found solution* \tilde{X}^* ;

354 objective value $\tilde{f}_\Theta(X)$. Hence, the surrogate objective values of the solutions in \mathcal{X} are
355 updated in each major COA iteration whenever the EC updates the surrogate suitability
356 function. The current best solution in \mathcal{X} , i.e., the solution with the highest surrogate
357 objective value, is denoted by \tilde{X}^* .

358 All feedback obtained from the users via the presented location scenarios is collected
359 and stored in the SMC in a hash map: Its set of keys, which we denote by K , is the set of
360 pairs (r, v) with $r \in R$, $v \in V$ for which suitability values $w_{r,v}$ have been obtained from
361 the users, and the respective values are the $w_{r,v}$.

362 Last but not least, through the FC we are also able to obtain upper bounds on
363 suitability values $w_{r,v}$, with $v \in V$, $r \in R$, as will be explained in Section 4.3. These
364 upper bounds are stored in the SMC as $w_{r,v}^{\text{UB}} \in [0, 1]$.

365 **4.3. Feedback Component**

366 The FC is responsible for extracting as much information as possible from the users
367 with as few interactions as necessary in order to not to fatigue them.

368 In the context of the COA framework, user interactions are understood as letting
369 a user evaluate (a small number of) *location scenarios*. Similar to a solution, a location
370 scenario is a subset of locations in V at which service stations are assumed to be opened.
371 In contrast to a solution the budget constraint (1) does not need to be respected and a
372 location scenario may therefore include an arbitrary number of service points. Recall
373 2 for an example how an interaction with the COA framework may look like from the
374 perspective of a user.

375 Let $S \subseteq V$ be such a location scenario provided to a user u in respect to one of
376 the user's SPRs $r \in R_u$. It is then assumed that the user returns as evaluation of the
377 scenario S either a best suited location $v_{r,S} \in S$ and the corresponding suitability value
378 $w(r, v_{r,S}) > 0$ or the information that none of the locations of the scenario S is suitable.

379 The latter case implies that $w_{r,v} = 0$ for all $v \in S$. In case multiple locations are equally
 380 well suited, we assume that the user selects one of them at random. It is assumed here
 381 that the suitability of a location w.r.t. an SPR can be specified by the user on a five-valued
 382 scale from zero, i.e., completely unsuitable, to one, i.e., perfectly suitable; a more fine
 383 grained evaluation would not make much practical sense.

384 Clearly, this definition of user interaction is simplified and idealized, in particular
 385 as we assume here that all users always give precise answers. In a real application, the
 386 uncertainty of user feedback and the possibility of misbehaving users who intentionally
 387 give misleading answers also need to be considered among other aspects. Moreover, it
 388 would be meaningful to extend the possibilities of user feedback. For example, users
 389 could be allowed to optionally rate more than one suitable locations for an SPR in one
 390 scenario or to make suggestions which locations to additionally include in a scenario as
 391 we considered it in [13].

392 In each iteration of COA, users get presented individual sets of location scenarios
 393 S_r for their service point requirements $r \in R$. These scenarios are compiled according to
 394 the following strategies.

395 Remember that location suitability values obtained from the users are later used in
 396 the EC for training the surrogate function \tilde{w}_Θ . Moreover, by enforcing that each user is
 397 required to select a best suited service point location in a presented location scenario for
 398 an SPR r , a suitability value indicated by the user for some location $v_{r,S}$ also serves as
 399 upper bound on the suitability values of all other locations in the location scenario S ;
 400 thus, $w_{r,v_{r,S}} \geq w_{r,v}, \forall v \in S$. By $w_{r,v}^{\text{UB}}$, the SMC maintains for each SPR $r \in R$, and each
 401 location $v \in V$ the so far best obtained upper bound on each $w_{r,v}$; initially, $w_{r,v}^{\text{UB}} = 1$.

402 Let $V_w(r) = \{v \mid w(r,v) > 0\}$ be the initially unknown set of locations that are
 403 actually relevant to a user $u \in U$ w.r.t. an SPR $r \in R_u$. A straight-forward strategy to
 404 identify this set is to iteratively present the user scenarios $S_r^V = \{v \in V \mid (r,v) \notin K\}$,
 405 containing all locations $v \in V$ for which no entry $(v,r) \in K$ exists yet, i.e., locations
 406 for which no suitability values are known yet w.r.t. r . Following this strategy, it can be
 407 ensured to identify a new location of $V_w(r)$ in every iteration of COA. Note, however,
 408 that it can only be guaranteed that $V_w(r)$ is completely known once the user returns that
 409 none of the locations in the last scenario S_r^V are suitable for r . Consequently, $V_w(r)$ will
 410 be completely known after $|V_w(r)| + 1$ user interactions.

Hence, an upper bound I_u^{UB} on the total number of required interactions with user
 u for completely identifying all relevant locations for all of his/her use cases is

$$I_u^{\text{UB}} = \sum_{r \in R_u} (|V_w(r)| + 1). \quad (12)$$

411 While this value is unknown in a real-world scenario, it allows us to establish a measure
 412 of quality on how well our strategy for presenting scenarios to users performs within
 413 our testing environments.

414 The same combination of two strategies for generating scenarios w.r.t. an SPR $r \in R$
 415 as in [16] is used. The first strategy generates scenarios according to the approach
 416 described above, i.e, $S_r^V = \{v \in V \mid (r,v) \notin K\}$. The second strategy generates scenarios
 417 $S_r^* = \{v \in \tilde{X}^* \mid (r,v) \notin K\}$ containing all locations from the current best solution that
 418 have not been rated yet w.r.t. r .

419 Note that for users generally only a fraction of the service point locations in V
 420 is actually relevant to one of their SPRs. Hence, when presenting a user $u \in U$ two
 421 scenarios for each of the user's SPRs every iteration the number of user interactions
 422 would quickly exceed I_u^{UB} . Therefore, in the first COA iteration a scenario S_r^V is generated
 423 for each $r \in R$, but in successive iterations, scenarios are only generated for subsets of
 424 R . More specifically from the second iteration onward, ζ^V and ζ^* percent of the SPRs
 425 $R_K = \{r \in R \mid \exists v \in V : (r,v) \notin K\}$ are randomly selected for generating scenarios
 426 according to S_r^V and S_r^* , respectively, with ζ^V and ζ^* being strategy parameters.

427 4.4. Evaluation Component

The EC processes the user feedback obtained from the FC and provides the means for evaluating candidate solutions without relying on users in particular within the OC. The exact objective function f from (2), which is based on the mostly unknown suitability values $w_{r,v}$ with $r \in R$, $v \in V$, is approximated by the surrogate objective function \tilde{f}_Θ , cf. (11), making use of the following *surrogate suitability function*

$$\tilde{w}_\Theta(r, v) = \begin{cases} w_{r,v} & \text{if } (r, v) \in K \\ \max(0, \min(w_{r,v}^{\text{UB}}, g_\Theta(r, v))) & \text{else.} \end{cases} \quad (13)$$

428 Generally speaking, g_Θ is here a learnable function with weight parameters Θ approxi-
429 mating $w_{r,v}$ for all unknown pairs $(r, v) \notin K$. The above definition thus ensures that \tilde{w}_Θ
430 always returns known values $w_{r,v}$ and otherwise respects lower bounds zero and upper
431 bounds $w_{r,v}^{\text{UB}}$, giving function g more freedom. Upper bounds $w_{r,v}^{\text{UB}}$ are initially set to one.
432 In Section 4.3 it was discussed how tighter upper bounds are derived.

433 Suitability values are approximated by exploiting similarities of SPRs among users.
434 In general we cannot expect that there exist users having the same needs in all respects,
435 i.e., the users have the very same use cases with the same demands. However, given
436 a sufficiently large user base it is realistic that there are users having similar SPRs and
437 associated preferences concerning suitable locations.

438 A popular collaborative filtering technique for exploiting similarities among user
439 preferences is *matrix factorization* [39], which we also apply here. Given an incomplete
440 matrix containing ratings $\mathcal{R} = (w_{i,j})_{i \in U, j \in P}$ for a set of users U over a set of products
441 P , the idea behind matrix factorization is to decompose this matrix into two smaller
442 matrices, a user/feature matrix ζ and a product/feature matrix ν , such that the product
443 of these two matrices approximates the original matrix. An unknown rating, i.e., a rating
444 not contained in the original matrix \mathcal{R} , can then be estimated as the dot product of the
445 corresponding feature vectors in matrix ζ and matrix ν , respectively.

Moreover, we also want to exploit the fact that only a small fraction of the locations in V is typically relevant for the SPR of a user and that unknown ratings are not missing at random. In our problem users are always asked to rate the most suitable location of a scenario. Therefore, known ratings tend to be biased towards more positive values while unrated locations are likely to have a low suitability for a user w.r.t. an SPR. A matrix factorization approach that takes such considerations into account has been suggested by [17]. Traditionally, the rating matrix \mathcal{R} is factorized by solving the optimization problem

$$\min_{\zeta, \nu} \sum_{i,j | w_{i,j} \in \mathcal{R}} E(w_{i,j}, \zeta_i \nu_j^T) + \rho(\zeta, \nu) \quad (14)$$

where E is a loss function for measuring the error between the actual and the predicted ratings and ρ is a regularization term. In [17] this minimization problem is expanded by adding a bias term for unknown ratings towards a certain value \hat{w} , i.e.,

$$\min_{\zeta, \nu} \sum_{i,j | w_{i,j} \in \mathcal{R}} E(w_{i,j}, \zeta_i \nu_j^T) + \alpha \sum_{i,j | w_{i,j} \notin \mathcal{R}} E(\hat{w}, \zeta_i \nu_j^T) + \rho(\zeta, \nu). \quad (15)$$

446 Parameter α controls the impact of this new term in the optimization. The authors show
447 for selected loss functions how this new optimization problem can be solved in the same
448 time complexity as the traditional optimization problem.

449 In order to apply matrix factorization for approximating suitability values $w_{r,v}$
450 in our case, we start from the sparsely filled matrix $W = (w_{r,v})_{(r,v) \in K}$ containing all
451 so far known suitability values. By factorizing W along the r dimension and the v
452 dimension on the basis of a feature set $F = \{1, \dots, \phi\}$, we obtain an SPR/feature matrix
453 $\zeta = (\zeta_{r,i})_{r \in R, i \in F}$ with $\zeta_{r,i} \in \mathbb{R}$ and a location/feature matrix $\nu = (\nu_{v,i})_{v \in V, i \in F}$ with
454 $\nu_{v,i} \in \mathbb{R}$. Feature vectors ζ_r describe the SPR r in terms of abstract features, while feature

455 vector v_v reflect the characteristics of locations v . In general, it is expected that SPRs with
 456 similar needs will have similar feature vectors in ξ , and locations with similar suitability
 457 characteristics will have similar feature vectors in v . The number of features ϕ is hereby
 458 a parameter that is chosen, e.g., in dependence of an estimation of the overall number of
 459 different service point requirements, and we assume it is considerably smaller than the
 460 overall number of SPRs as well as the number of locations n . As unknown suitability
 461 values are more likely zero than being greater than zero, we set the bias target $\hat{w} = 0$.

Having obtained matrices ξ and v , an unknown value of W is approximated by the dot product of the respective feature vectors rounded to the nearest of the five discrete suitability values we defined, i.e.,

$$g_{\Theta}(r, v) = \lfloor 4 \cdot \xi_r v_v^T + 0.5 \rfloor / 4. \quad (16)$$

462 The trainable parameters of g_{Θ} are therefore $\Theta = (\xi, v)$.

Our loss function for the matrix factorization is

$$\min \sum_{(r,v) \in K} (w_{r,v} - \xi_r v_v^T)^2 + \alpha \sum_{(r,v) \notin K} (\xi_r v_v^T)^2 + \lambda (\|\xi_r\|^2 + \|v_v\|^2), \quad (17)$$

463 and randomized block coordinate descent [47] is used to minimizing it.

464 4.5. Optimization Component

465 Recall that the OC is performed in each major iteration of the framework and makes
 466 use of the current surrogate objective function \tilde{f}_{Θ} provided by the EC, whose weights
 467 Θ do not change during each individual call of the OC. The OC is thus supposed to
 468 return an optimal or close-to-optimal solution to our problem w.r.t. the current surrogate
 469 objective function.

470 In our implementation of the OC, we apply a general purpose MILP solver to the
 471 MILP formulation already presented in Section 3, Equations (3)–(10), however suitability
 472 values are approximated by the surrogate suitability function \tilde{w}_{Θ} . Note that for improved
 473 scalability, a metaheuristic approach might also be used as optimization core as it is not
 474 necessary to find an optimal solution in each iteration. However, due to the complexity
 475 of the objective function of the GSPDP, such a metaheuristic requires significant effort to
 476 be able to scale well to larger instances. As the development of such a heuristic would
 477 go beyond the scope of this paper, we therefore leave this task for future work.

478 5. Test Cases

479 In the following it is described how test instances for evaluating COA have been
 480 generated. Instead of testing with real users, user interaction is simulated in an idealized
 481 manner in certain test cases in order to analyze the strengths and weaknesses of the
 482 framework with a focus on the algorithmic aspects. The considered test instances are
 483 of three groups. The first two groups are purely artificial test instances inspired by
 484 the location planning of stations for electric vehicle charging, denoted by EVC, and
 485 for (station-based) car sharing systems, denoted by CSS, respectively. While in group
 486 EVC each use case has one SPR, there are always two SPRs per use case in CSS. The
 487 third group of test instances is designed similarly to group CSS, also addressing the
 488 car sharing scenario, but the instances are generated from real-world taxi trip data of
 489 Manhattan; this group is therefore called MAN. Note that COA intentionally does not
 490 make use of geographic information in any of its components. Therefore, modeling
 491 preferences of users for our instances in dependence of the proximity to service point
 492 locations does not provide COA any advantage for finding an optimized solution.

493 All of our benchmark instances are available online at [https://www.ac.tuwien.ac.
 494 at/research/problem-instances/#spdp](https://www.ac.tuwien.ac.at/research/problem-instances/#spdp).

495 5.1. Artificial Test Instance Groups EVC and CSS

496 Test instances from the groups EVC and CSS are generated with the same approach.
 497 The n possible locations for service stations are randomly distributed in the Euclidean
 498 plane with coordinates $\text{coord}(v)$, $v \in V$, chosen uniformly from the grid $\{0, \dots, L-1\}^2$,
 499 with $L = \lceil 10\sqrt{n} \rceil$. The fixed costs z_v^{fix} as well as the variable costs z_v^{var} for setting up a
 500 service station at each location $v \in V$ are uniformly chosen at random from $\{50, \dots, 100\}$.
 501 The budget is assumed to be $B = \lceil 7.5 \cdot n \rceil$ so that roughly 10% of the stations with
 502 average costs can be expected to be opened.

503 The number of use cases for each user $u \in U$ is chosen randomly according to
 504 a shifted Poisson distribution with offset one, expected value three, and a maximum
 505 value of five, i.e., the number of use cases never exceeds five. Each of these use cases
 506 $c \in C_u$ is associated with an individual demand $D_{u,c}$ randomly chosen from $\{5, \dots, 50\}$
 507 and, depending on the benchmark group, with one (EVC) or two (CSS) SPRs.

Each SPR $r \in R_{u,c}$ of a use case c also is associated with a particular geographic
 location $q_r \in \{0, \dots, L-1\}^2$. In order to model similarities in the users' SPRs, these
 locations are selected in the following correlated way. First ten *attraction points* A with
 uniform random coordinates are selected from $\{0, \dots, L-1\}^2$. Then, each use case
 location is derived by randomly choosing one of these attraction points $(a_x, a_y) \in A$ and
 adding a small individual offset to the coordinates, i.e.,

$$q_r = (\lfloor \mathcal{N}(a_x, \sigma_v) \rfloor, \lfloor \mathcal{N}(a_y, \sigma_v) \rfloor), \quad (18)$$

508 where $\mathcal{N}(\cdot, \cdot)$ denotes a random value sampled from a normal distribution with the
 509 respectively given mean value and standard deviation σ_v . If obtained coordinates are
 510 not in $\{0, \dots, L-1\}^2$ a new attraction point is chosen and the deviation is re-sampled.

A service point location $v \in V$ receives a rating w.r.t. an SPR r according to a
 sigmoidal decay function applied to the Euclidean distance, and is also perturbed by a
 Gaussian noise with a standard deviation of σ_r :

$$w'_{r,v} = \mathcal{N}\left(\frac{1}{1 + 6e^{0.5\|q_r - \text{coord}(v)\| - 6}}, \sigma_r\right). \quad (19)$$

511 The parameters of the sigmoid function are chosen so that $w'_{r,v}$ decreases as the dis-
 512 tance between v and q_r increases and becomes approximately zero at a distance larger
 513 than twelve. Additionally, as motivated in Section 3, we discretize the rating $w'_{r,v}$ by
 514 rounding to the closest value in $\{0, 0.25, 0.5, 0.75, 1\}$, obtaining $w_{r,v}$. Hence, $w_{r,v} =$
 515 $\lfloor 4 \cdot \min(1, \max(0, w'_{r,v})) + 0.5 \rfloor / 4$.

516 Six sets of 30 benchmark instances were generated for EVC as well as CSS. As
 517 detailed in Table 1, these sets consider $n \in \{100, 200, 300\}$ potential service point loca-
 518 tions in combination with different numbers of users and two different settings for the
 519 standard deviations of the Gaussian perturbations σ_v and σ_r . Note that parameters σ_v
 520 and σ_r control how similar suitability values for locations of SPRs generated from the
 521 same attraction point are. The larger σ_v and σ_r , the more different are the preferences of
 522 the users. Hence, we have chosen two different settings for σ_v and σ_r to show how COA
 523 behaves under conditions in which preferences of users towards locations for service
 524 points have a higher and lower similarity, respectively. Values for σ_v and σ_r have been
 525 determined experimentally in preliminary tests. In the following we will denote instance
 526 sets primarily by the pair (n, m) .

527 5.2. Manhattan Test Instances

528 Next to the above described purely artificial benchmark instances we also derive
 529 benchmark instances from real-world yellow taxi trip data of Manhattan. As in CSS,
 530 MAN instances have two SPRs per use case. The underlying street network G of the
 531 instances corresponds to the street network graph of Manhattan provided by the Julia

Table 1: Main parameters of the EVC and CSS instance sets of groups EVC and CSS. Each row represents a set of 30 instances.

(n, m)	σ_v	σ_r
(100, 500)	3.0	0.03
(100, 1000)	5.0	0.15
(200, 1000)	3.0	0.03
(200, 2000)	5.0	0.15
(300, 1500)	3.0	0.03
(300, 3000)	5.0	0.15

532 package LightOSM¹. Taxi trips have been extracted from the 2016 Yellow Taxi Trip
 533 Data². The taxi data set was first preprocessed by removing all trips with invalid data
 534 and trips made on a weekend. Furthermore, we have also removed all trips which
 535 do not start as well as end in Manhattan. For taxi trips within the months January to
 536 July geographic pickup and drop-off coordinates of customers are recorded in the data
 537 set. Each of these coordinates has been extracted and mapped to the geographically
 538 closest vertex in G , resulting in a list of pairs of vertices $Q \subseteq V(G) \times V(G)$. Next, as
 539 the similarity of users in our instances depends on their geographic proximity, we have
 540 reduced Q by considering only the ten taxi zones with the highest total number of
 541 pickups and drop-offs of customers, resulting in a total of approximately two million
 542 taxi trips. Geographic information of the taxi zones of Manhattan has been obtained
 543 from <https://data.cityofnewyork.us/Transportation/NYC-Taxi-Zones/d3c5-ddgc>. The
 544 left side of Figure 4 provides a visualization of the selected taxi zones.

545 The set of potential service point locations V has been chosen randomly from
 546 vertices of G that are located in the considered taxi zones. The fixed costs z_v^{fix} as well as
 547 the variable costs z_v^{var} for setting up a service station at each location $v \in V$ are uniformly
 548 chosen at random from $\{50, \dots, 100\}$.

The number of use cases for each user $u \in U$ is again chosen randomly according
 to a shifted Poisson distribution with offset one, expected value three, and a maximum
 value of five. Each of these use cases $c \in C_u$ is associated with an individual demand
 $D_{u,c}$ randomly chosen from $\{5, \dots, 50\}$ and the two SPRs representing the origin and
 destination of a trip chosen from Q uniformly at random. A rating for an SPR r is
 calculated for each $v \in V$ via the sigmoidal decay function

$$w'_{r,v} = \frac{1}{1 + 10e^{0.01\text{sp}(r,v)} - 6} \quad (20)$$

549 where $\text{sp}(r, v)$ refers to the length of the shortest path between location v and the SPR
 550 r in the street network graph G . The parameters of this function have been chosen in
 551 such a way that service point locations within a distance of approximately 600 meters to
 552 r are relevant for the SPR. Finally, the discretized suitability value $w_{r,v}$ is again obtained
 553 by $w_{r,v} = \lfloor 4 \cdot \min(1, \max(0, w'_{r,v})) + 0.5 \rfloor / 4$. The right side of Figure 4 shows the
 554 distribution of SPR locations as well as potential service point locations for an example
 555 instance.

556 The MAN benchmark group consists of 30 instances in total with each instance
 557 having 100 potential service point locations and 2000 users. Additionally, each instance
 558 will be evaluated with different budget levels $b [\%] \in \{30, 50, 70\}$ such that about b
 559 percent of the stations considering average costs can be opened, i.e, the actual budget for
 560 each instance is calculated as $B = \lceil b \cdot 0.75 \cdot n \rceil$.

¹ <https://github.com/DeloitteDigitalAPAC/LightOSM.jl>

² <https://data.cityofnewyork.us/Transportation/2016-Yellow-Taxi-Trip-Data/k67s-dv2t>

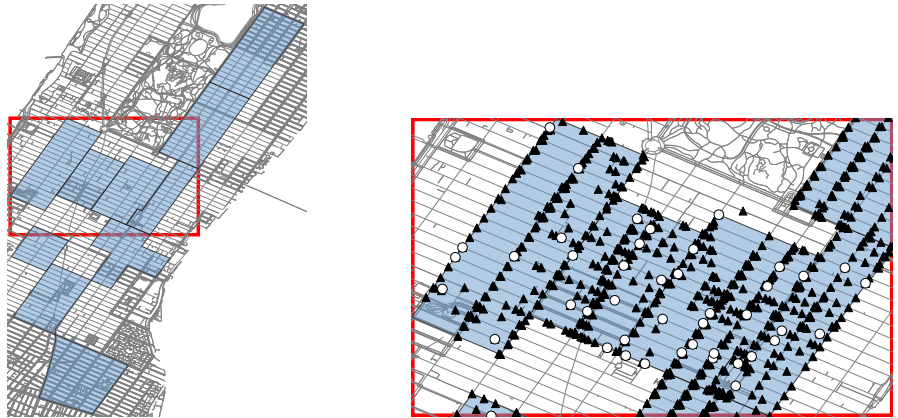


Figure 4. Left: The considered ten taxi zones of Manhattan with the highest number of pickups and drop-offs. Right: Exemplary distribution of SPR locations (black triangles) and potential service point locations (white points).

561 6. Results

562 The COA framework including the FC were implemented in Python 3.8. For the
 563 matrix factorization of the EC we adapted the C++ implementation of [17] provided on
 564 Github³. The parameterization of the COA components have been determined through
 565 preliminary tests on an independent set of instances. For all test runs the weighting for
 566 unknown suitability values α of the matrix factorization has been set to one. Moreover,
 567 the number of features considered in the matrix factorization is set to ten for all test runs.
 568 The parameters ζ^V and ζ^* for controlling the number of scenarios generated according
 569 to each strategy in the FC have been set to 0.5 and 0.1, respectively. Finally, Gurobi 9.1⁴
 570 was used to solve the MILP models in the OC. In each COA iteration a time limit of ten
 571 minutes has been set for solving the MILP. If the MILP was not solved to optimality
 572 within this time limit, the best found solution was used. All test runs have been executed
 573 on an Intel Xeon E5-2640 v4 2.40GHz machine in single-threaded mode with a global
 574 time limit of four hours per run. Note however, that all runs terminated within this
 575 time limit once all relevant locations had been discovered. Since in contrast to COA
 576 we have full knowledge of our test instances, we are also able to calculate optimal
 577 reference solutions for each instance. Hence, by $f(x_{\text{opt}})$ we denote the objective value of
 578 a respective optimal solution x_{opt} .

579 To characterize the amount of user interaction performed by COA, we consider
 580 the total number of scenarios evaluated by a user $u \in U$ in relation to the upper bound
 581 of required interactions I_u^{UB} , cf. Section 4.3. Let I_u be the number of user interactions
 582 of user $u \in U$ performed within COA to generate some solution. Then, $I = 100\% \cdot$
 583 $(\sum_{u \in U} I_u / I_u^{\text{UB}}) / m$, refers to the relative average number of performed user interactions
 584 relative to I_u^{UB} over all users. Note that since scenarios are presented only to a fraction
 585 of users in every iteration, the average number of user interactions at each iteration of
 586 COA varies even for instances within the same benchmark group. Hence, in order to
 587 reasonably study results for each of our benchmark groups, we aggregate respective
 588 results to our instances at various *interaction levels* ψ by selecting for each instance the
 589 COA iteration at which I is largest but does not exceed ψ . Note that for some instances
 590 smaller levels of ψ are already exceeded in the first iteration of COA. Hence, in the
 591 following we only consider interaction levels for an instance group for which results to
 592 all corresponding instances exist.

593 Note further that the user interaction levels can also be interpreted as the average in-
 594 formation known about a user. This interpretation allows us to draw a direct comparison

³ <https://github.com/rdevooght/MF-with-prior-and-updates>

⁴ <https://www.gurobi.com/>

595 to traditional approaches for distributing service points in which information about the
 596 demands of the users is determined in advance. Each result at a certain interaction level
 597 can also be interpreted as the result of such a traditional approach with a certain level
 598 of knowledge about the users. However, to the best of our knowledge there exists no
 599 data about suitability values in other work. Additionally, for a fair comparison between
 600 COA and other approaches from literature one would have to also take into account
 601 the costs required for obtaining said information about the users. Therefore, comparing
 602 COA to other approaches from literature seems to be not possible without an extensive
 603 study on suitability values of users or a complex simulation of users based on various
 604 assumptions that can heavily influence the outcome of such a comparison.

605 First, we want to show how the quality of incumbent solutions develops as the
 606 number of user interactions increases during a COA run. For this purpose, we calculate
 607 the optimality gap for a solution x obtained from COA as $\text{gap} = 100\% \cdot (f(x_{\text{opt}}) -$
 608 $f(x))/f(x_{\text{opt}})$. Figure 5 shows the average optimality gaps of solutions to each of our
 609 benchmark sets against the interaction levels ψ . The results are grouped by σ_v and σ_r to
 additionally compare instances groups with similar user behavior.

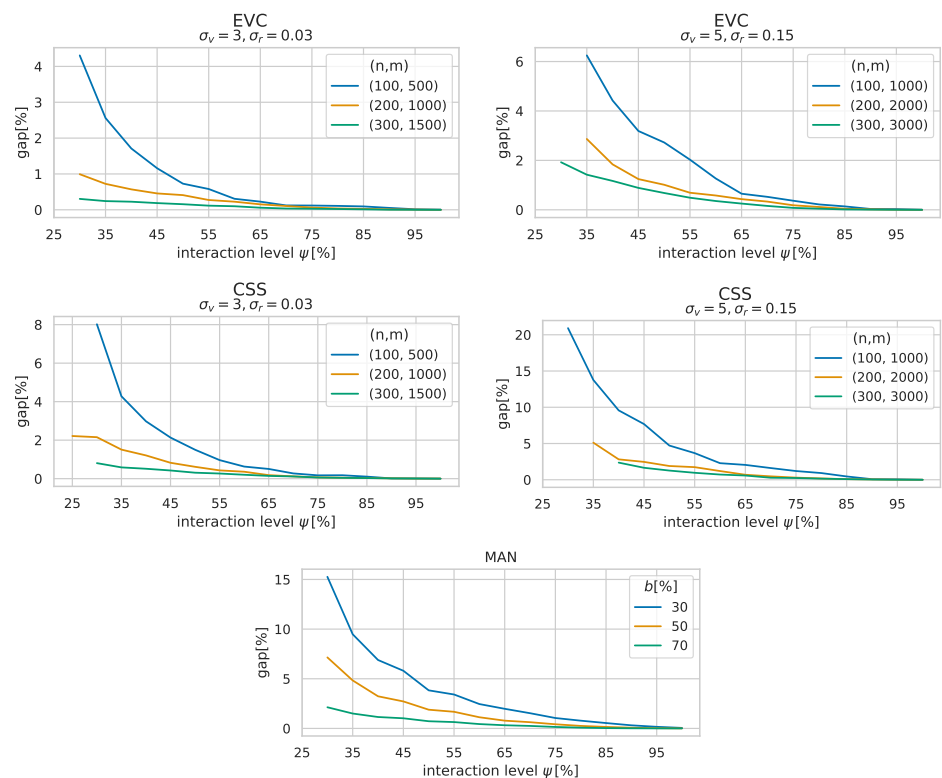


Figure 5. Development of average optimality gaps with an increasing number of user interactions for each benchmark instance set.

610 Recall that the number of attraction points is the same for all EVC and CSS instances.
 611 Therefore, for instances with a higher number of users it is generally easier to find better
 612 solutions as there are more users that prefer the same locations. The plots show that in
 613 all cases solutions generally improve quickly with an increasing interaction level and
 614 close to optimal solutions can be obtained well before identifying all the users' relevant
 615 locations. Specifically, at a user interaction level of 50% the solutions generated by COA
 616 feature optimality gaps of 1.45% on average. An exception of this observation are the
 617 MAN instances with $b = 30\%$. For these generated solutions do not reach an optimality
 618 gap below 1% before $\psi = 80\%$ on average. Moreover, the figure also shows that the
 619 solutions to MAN instances generally converge notably slower than the solutions to
 620 EVC and CSS instances. This behavior is likely caused by the weaker correlation of
 621

622 user preferences in the MAN instances and the way how the FC generates scenarios
 623 presented to the users, specifically the aspect that locations important to the individual
 624 users are tried to be identified first. Locations important to individual users might not
 625 necessarily be the best locations to add to a solution, especially if there is a lower number
 626 of users with similar preferences. Consequently, the strategies based on which scenarios
 627 are generated may still have some room for improvement for such cases. Instead of
 628 primarily identifying locations important to users, targeting locations in relation to the
 629 current best solution with a higher emphasis might be a more expedient approach here.

Note that an increased number of user interactions does not only imply a larger trainings set for the surrogate function but also results in better upper bounds $w_{r,v}^{\text{UB}}$ for locations $v \in V$ w.r.t. to an SPR $r \in R$. Therefore, to gain a better understanding of how much the surrogate function actually contributes to finding an optimized solution, we study what happens when the learning surrogate suitability function \tilde{w}_Θ is replaced by the naive function with no learning capabilities

$$\tilde{w}_{\text{bl}}(r, v) = \begin{cases} w_{r,v} & \text{if } (r, v) \in K \\ 0 & \text{else.} \end{cases} \quad (21)$$

630 In the following we refer to our original COA implementation with the surrogate function
 631 \tilde{w}_Θ as $\text{COA}[\tilde{w}_\Theta]$ and denote the implementation with the naive function \tilde{w}_{bl} as $\text{COA}[\tilde{w}_{\text{bl}}]$.
 632 A comparison between $\text{COA}[\tilde{w}_\Theta]$ and $\text{COA}[\tilde{w}_{\text{bl}}]$ is shown in Table 2. Each table cell
 633 shows the average optimality gaps of solutions to the respective instance group at the
 634 specified interaction levels ψ . The better results among $\text{COA}[\tilde{w}_\Theta]$ and $\text{COA}[\tilde{w}_{\text{bl}}]$ are
 635 printed bold. Additionally, as the standard deviations w.r.t. the optimality gaps are
 636 quite large, see Figure 6, we have also applied a one-sided Wilcoxon signed-rank test to
 637 determine for each group whether the difference in optimality gaps is significant or not.
 638 Instance groups for which the Wilcoxon test has assessed at a 95% confidence interval
 639 that either $\text{COA}[\tilde{w}_\Theta]$ or $\text{COA}[\tilde{w}_{\text{bl}}]$ has produced better optimality gaps are marked with
 640 an asterisk.

641 The table shows that especially for the CSS and MAN instances $\text{COA}[\tilde{w}_\Theta]$ generates
 642 significantly better results at almost all interaction levels ψ than $\text{COA}[\tilde{w}_{\text{bl}}]$. While for the
 643 EVC instances the average optimality gaps w.r.t. $\text{COA}[\tilde{w}_\Theta]$ are lower than the average
 644 optimality gaps w.r.t. $\text{COA}[\tilde{w}_{\text{bl}}]$, there are instance groups for which no significant
 645 difference between the optimality gaps can be determined. However, there is no instance
 646 group for which $\text{COA}[\tilde{w}_{\text{bl}}]$ produced significantly better results than COA with \tilde{w}_Θ
 647 over all user interaction thresholds. It can be observed that at very low levels of user
 648 interaction $\text{COA}[\tilde{w}_\Theta]$ and $\text{COA}[\tilde{w}_{\text{bl}}]$ seem to be equally strong. However, as the amount
 649 of collected of user feedback increases, $\text{COA}[\tilde{w}_\Theta]$ quite quickly outperforms $\text{COA}[\tilde{w}_{\text{bl}}]$.

650 Figure 6 gives a visual comparison between $\text{COA}[\tilde{w}_\Theta]$ and $\text{COA}[\tilde{w}_{\text{bl}}]$ for selected
 651 instance groups and not only shows average optimality gaps but also respective standard
 652 deviations around the mean values as shaded areas. The figure confirms that the average
 653 gaps produced by $\text{COA}[\tilde{w}_\Theta]$ are generally lower than those of $\text{COA}[\tilde{w}_{\text{bl}}]$ but also shows
 654 that the standard deviations are quite large in general for both approaches. But as COA
 655 progresses and the quality of the solutions improves, the standard deviations decrease
 656 as well.

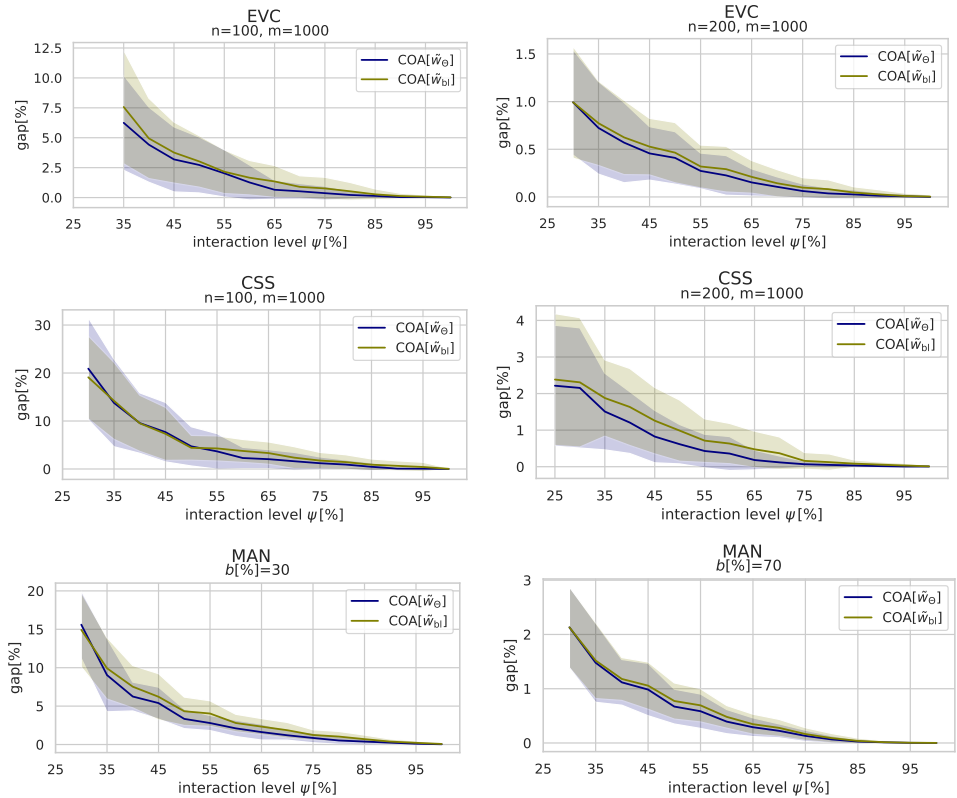
657 To further investigate the learning capabilities of the surrogate function, we now
 658 look at the mean squared error (MSE) of \tilde{w}_Θ in respect to the known exact values w . The
 659 left plots in Figure 7 show the development of this MSE calculated over all suitability
 660 values that are not known yet by COA for all instance groups. It can be seen that the
 661 MSE is generally small and approaches zero rather quickly. The reason for such small
 662 values can be found in the matrix factorization model used in the EC, which adds a bias
 663 for unknown suitability values towards zero as users typically only have a small number
 664 of locations with positive suitability values for each of their SPRs. Consequently, the
 665 MSE is distorted by the large number suitability values that are zero.

Table 2: Average optimality gaps obtained by COA using the surrogate suitability functions with (\tilde{w}_Θ) and without learning capabilities (\tilde{w}_{bl}) at different interaction levels.

		EVC											
(n,m)		(100,500)		(100,1000)		(200,1000)		(200,2000)		(300,1500)		(300,3000)	
ψ		COA[\tilde{w}_Θ]	COA[\tilde{w}_{bl}]	COA[\tilde{w}_Θ]	COA[\tilde{w}_{bl}]	COA[\tilde{w}_Θ]	COA[\tilde{w}_{bl}]	COA[\tilde{w}_Θ]	COA[\tilde{w}_{bl}]	COA[\tilde{w}_Θ]	COA[\tilde{w}_{bl}]	COA[\tilde{w}_Θ]	COA[\tilde{w}_{bl}]
30%		4.31	4.03	-	-	0.99	0.99	-	-	0.30	0.32	1.93	1.94
40%		1.71	2.00	4.42	4.95	0.57	0.62	1.84	2.06	0.23	0.23	1.17*	1.31
50%		0.73*	1.11	2.72	3.03	0.41	0.46	1.01*	1.44	0.16	0.16	0.68*	0.86
60%		0.31*	0.69	1.27*	1.66	0.23*	0.29	0.58*	0.91	0.10	0.09	0.36*	0.49
70%		0.12*	0.42	0.53*	0.90	0.11	0.14	0.33*	0.50	0.04*	0.06	0.16*	0.30
80%		0.11*	0.18	0.22*	0.53	0.04*	0.08	0.11*	0.21	0.02	0.04	0.05*	0.10
90%		0.05	0.11	0.03*	0.13	0.01	0.03	0.02*	0.06	0.00*	0.01	0.01*	0.02

		CSS											
(n,m)		(100,500)		(100,1000)		(200,1000)		(200,2000)		(300,1500)		(300,3000)	
ψ		COA[\tilde{w}_Θ]	COA[\tilde{w}_{bl}]	COA[\tilde{w}_Θ]	COA[\tilde{w}_{bl}]	COA[\tilde{w}_Θ]	COA[\tilde{w}_{bl}]	COA[\tilde{w}_Θ]	COA[\tilde{w}_{bl}]	COA[\tilde{w}_Θ]	COA[\tilde{w}_{bl}]	COA[\tilde{w}_Θ]	COA[\tilde{w}_{bl}]
30%		8.02	7.60	20.92	19.11*	2.15	2.31	-	-	0.81	0.82	-	-
40%		2.98*	4.28	9.57	9.52	1.21*	1.63	2.81*	3.78	0.51	0.52	2.36*	2.64
50%		1.50*	2.41	4.72	4.41	0.62*	0.99	1.90*	2.77	0.31*	0.38	1.27*	1.80
60%		0.63*	1.51	2.29*	3.76	0.36*	0.63	1.20*	1.83	0.20*	0.26	0.72*	1.15
70%		0.27*	0.51	1.61*	2.36	0.12*	0.37	0.47*	1.09	0.11*	0.15	0.28*	0.59
80%		0.18*	0.43	0.92*	1.44	0.05*	0.12	0.18*	0.46	0.04*	0.07	0.15*	0.29
90%		0.01*	0.14	0.08*	0.65	0.02*	0.06	0.05*	0.15	0.01	0.02	0.03*	0.07

		MAN					
b		30%			70%		
ψ		COA[\tilde{w}_Θ]	COA[\tilde{w}_{bl}]	COA[\tilde{w}_Θ]	COA[\tilde{w}_{bl}]	COA[\tilde{w}_Θ]	COA[\tilde{w}_{bl}]
30%		15.61	14.93	7.02	7.28	2.13	2.13
40%		6.25*	7.53	3.01*	3.46	1.12	1.18
50%		3.34*	4.33	1.63*	2.14	0.67*	0.77
60%		2.10*	2.80	0.93*	1.32	0.39*	0.48
70%		1.20*	1.86	0.46*	0.80	0.22*	0.28
80%		0.52*	1.04	0.18*	0.33	0.07*	0.09
90%		0.24*	0.38	0.04*	0.10	0.01	0.01

Figure 6. Average optimality gaps with standard deviations as shaded areas obtained by COA using the surrogate suitability functions with learning capabilities (\tilde{w}_Θ) and without (\tilde{w}_{bl}) plotted over the interaction level.

666 Therefore, the plots on the right side of Figure 7 show average mean squared errors
667 calculated only over all *positive* suitability values that are not known yet; we denote
668 this error by MSE+. This measure gives a clearer picture on how the surrogate function
669 continuously improves in all cases with an increasing amount of gained knowledge. At

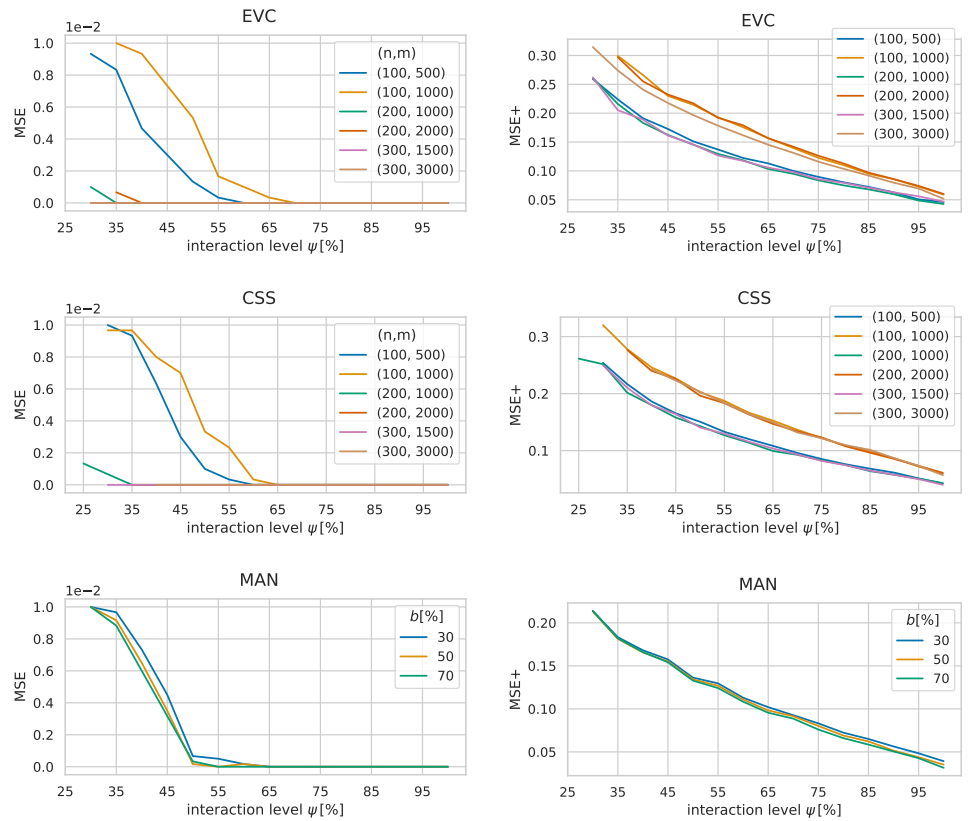


Figure 7. Development of average MSEs of \tilde{w}_Θ over all so far unknown suitability values (left) and all so far unknown *positive* suitability values (right) for all benchmark sets.

670 the start of the algorithm the MSEs of the benchmark groups are between 0.2 and 0.3 on
 671 average and go towards zero almost linearly with the interaction level. Note that neither
 672 the size of an instance nor the given budget seem to have a significant impact on the size
 673 of the errors. Additionally, the figure also highlights how the instance parameters σ_v and
 674 σ_r impact the similarity of user preferences as the MSEs for instances with $\sigma_v = 5$ and
 675 $\sigma_r = 0.15$ are generally larger than the MSEs for instances with $\sigma_v = 3$ and $\sigma_r = 0.03$.

676 Finally, in Table 3 we also compare $\text{COA}[\tilde{w}_\Theta]$ to the COA implementation using the
 677 surrogate function \tilde{w}'_Θ introduced in [16], henceforth referred to as $\text{COA}[\tilde{w}'_\Theta]$. While \tilde{w}'_Θ
 678 is also based on a matrix factorization model, this model does not take into account that
 679 user data is not missing at random.

680 Each table cell shows the average optimality gaps of solutions to the respective
 681 instance set at the specified interaction level ψ . The better results among $\text{COA}[\tilde{w}_\Theta]$
 682 and $\text{COA}[\tilde{w}'_\Theta]$ are printed bold. A one-sided Wilcoxon signed-rank test was used to
 683 determine for each instance set whether the difference in optimality gaps is significant
 684 or not. Entries for which the Wilcoxon test has assessed at a 95% confidence level that
 685 either $\text{COA}[\tilde{w}_\Theta]$ or $\text{COA}[\tilde{w}'_\Theta]$ has produced better optimality gaps are marked with an
 686 asterisk. It can be observed that for lower levels of user interaction, solutions generated
 687 by $\text{COA}[\tilde{w}'_\Theta]$ exhibit extremely high optimality gaps. However, the higher the number
 688 of user interactions, the more $\text{COA}[\tilde{w}'_\Theta]$ can catch up with $\text{COA}[\tilde{w}_\Theta]$. Though, most of
 689 the time $\text{COA}[\tilde{w}_\Theta]$ still dominates $\text{COA}[\tilde{w}'_\Theta]$. Summarizing, it can be concluded that the
 690 new matrix factorization model is a significant improvement over our previous model
 691 \tilde{w}'_Θ resulting in $\text{COA}[\tilde{w}_\Theta]$ generating better solutions with fewer user interactions than
 692 $\text{COA}[\tilde{w}'_\Theta]$ most of the time.

693 7. Conclusion and Future Work

694 In this paper the previously introduced Cooperative Optimization Algorithm was
 695 generalized to be applicable to more application scenarios and to larger instances with

Table 3: Average optimality gaps of solution from COA $[\tilde{w}_\Theta]$ and COA $[\tilde{w}'_\Theta]$, where the latter utilizes the former surrogate function \tilde{w}'_Θ from [16].

		EVC											
(n, m)	(100, 500)		(100, 1000)		(200, 1000)		(200, 2000)		(300, 1500)		(300, 3000)		
	COA $[\tilde{w}'_\Theta]$	COA $[\tilde{w}_\Theta]$	COA $[\tilde{w}'_\Theta]$	COA $[\tilde{w}_\Theta]$	COA $[\tilde{w}'_\Theta]$	COA $[\tilde{w}_\Theta]$	COA $[\tilde{w}'_\Theta]$	COA $[\tilde{w}_\Theta]$	COA $[\tilde{w}'_\Theta]$	COA $[\tilde{w}_\Theta]$	COA $[\tilde{w}'_\Theta]$	COA $[\tilde{w}_\Theta]$	
30%	81.89	4.31*	-	-	85.20	0.99*	-	-	82.14	0.30*	95.53	1.93*	
40%	16.07	1.71*	34.82	4.42*	3.22	0.57	32.79	1.84*	9.08	0.23	23.21	1.17*	
50%	1.95	0.73*	3.91	2.72*	0.35*	0.41	1.51	1.01*	0.13*	0.16	0.87	0.68*	
60%	0.62	0.31*	2.20	1.27*	0.24	0.23	0.76	0.58*	0.09	0.10	0.48	0.36*	
70%	0.46	0.12*	0.70	0.52	0.13	0.11	0.45	0.33*	0.04	0.04	0.24	0.16*	
80%	0.22	0.11*	0.31	0.22	0.06	0.04*	0.17	0.11*	0.02	0.02	0.11	0.05*	
90%	0.09	0.05	0.09	0.03*	0.02	0.01	0.05	0.02*	0.01	0.00	0.02	0.01*	

		CSS											
(n, m)	(100, 500)		(100, 1000)		(200, 1000)		(200, 2000)		(300, 1500)		(300, 3000)		
	COA $[\tilde{w}'_\Theta]$	COA $[\tilde{w}_\Theta]$	COA $[\tilde{w}'_\Theta]$	COA $[\tilde{w}_\Theta]$	COA $[\tilde{w}'_\Theta]$	COA $[\tilde{w}_\Theta]$	COA $[\tilde{w}'_\Theta]$	COA $[\tilde{w}_\Theta]$	COA $[\tilde{w}'_\Theta]$	COA $[\tilde{w}_\Theta]$	COA $[\tilde{w}'_\Theta]$	COA $[\tilde{w}_\Theta]$	
30%	80.12	8.02*	98.68	20.92*	86.58	2.15*	-	-	69.78	0.81*	-	-	
40%	13.80	2.98*	24.73	9.57*	1.38	1.21	13.93	2.81*	3.84	0.51	6.17	2.36*	
50%	2.34	1.50	7.31	4.72*	0.77	0.62	2.66	1.90*	0.33	0.31	4.73	1.27	
60%	1.83	0.63*	2.53	2.29	0.49	0.36*	1.56	1.20*	0.22	0.20	0.83	0.72	
70%	0.66	0.27*	1.91	1.61	0.21	0.12	0.74	0.47*	0.12	0.11	0.59	0.28*	
80%	0.12	0.18	0.99	0.92	0.10	0.05*	0.42	0.18*	0.04	0.04	0.23	0.15*	
90%	0.08	0.01*	0.45	0.08*	0.04	0.02	0.20	0.05*	0.02	0.01	0.13	0.03*	

		MAN					
b	ψ	30%		50%		70%	
		COA $[\tilde{w}'_\Theta]$	COA $[\tilde{w}_\Theta]$	COA $[\tilde{w}'_\Theta]$	COA $[\tilde{w}_\Theta]$	COA $[\tilde{w}'_\Theta]$	COA $[\tilde{w}_\Theta]$
30%	99.78	15.61*	99.83	7.02*	99.83	2.13*	
40%	13.84	6.25*	3.97	3.01*	1.15	1.12	
50%	8.46	3.34*	1.93	1.63*	0.63	0.67	
60%	3.18	2.10*	0.89	0.93	0.35	0.39	
70%	1.86	1.20*	0.64	0.46*	0.26	0.22	
80%	1.15	0.53*	0.34	0.18*	0.12	0.07*	
90%	0.47	0.24*	0.14	0.04*	0.03	0.01*	

696 hundreds of potential service station locations and thousands of users. New application
697 scenarios include in particular those in which the fulfillment of a single demand depends
698 on more than one suitably located service points as it is the case in station-based bike
699 and care sharing. Results on artificial and real world inspired instances show how the
700 solution quality improves as the amount of user feedback increases and that a near
701 optimal solution is reached for most instances with a reasonably low amount of user
702 interactions. To characterize the amount of user interaction performed by COA, we
703 have established an upper bound on the maximum number of non-redundant user
704 interactions and introduced the notion of user interaction levels. Solutions generated
705 by COA feature optimality gaps of 1.45% on average at an interaction level of 50%.
706 Furthermore, we could clearly observe that the matrix factorization based surrogate
707 model is able to learn preferences of individual users from users with similar interests.
708 More specifically, we made use of an advanced matrix factorization model which takes
709 into account that user data is not missing at random. In fact, users are always asked to
710 rate the most suitable location of a scenario, if one exists. The experimental comparison
711 indeed confirmed the benefits of this new model over the original one, especially when
712 the interaction level is still low. Using the new matrix factorization model, COA is able
713 to generate better solutions with fewer known user preferences than before. Also note
714 that while we achieve our best results with the matrix factorization based surrogate
715 model, the results also show that COA already works reasonable even without learning
716 user preferences.

717 However, there is still potential left for future improvements. In our COA imple-
718 mentation, the strategies by which scenarios for users are generated favor the selection
719 of unrated locations that may be important for individual users but not necessarily for a
720 global optimal solution. In order to quickly find a good solution by the optimization it
721 is important for our surrogate function to have higher accuracy for locations that have
722 the potential to actually appear in a globally optimal solution. Otherwise, finding a near
723 optimal solution requires a larger amount of user interactions as we have observed in
724 our results on the Manhattan instances. In order to improve the scenario generation
725 strategies, it seems natural to enrich the feedback component (FC) with knowledge not
726 only from the evaluation component (EC) but also from the optimization component
727 (OC). As the OC finds optimized solutions via a MILP, utilizing dual solution informa-

728 tion such as reduced costs or performing a sensitivity analysis might be a promising
729 direction.

730 It would also be interesting to further improve the scalability of COA. While a time
731 limit of ten minutes per MILP was still sufficient for solving our benchmark instances,
732 the OC is the main bottleneck of COA w.r.t. computation times. On the one hand, one can
733 resort to heuristic optimization approaches in the OC. On the other hand, hierarchical
734 clustering and multilevel refinement strategies as applied in the context of planning a
735 bike sharing system in [2] appear promising.

736 COA was applied for generating solutions to instances of the General Service Point
737 Distribution Problem (GSPDP). While we have proven the GSPDP to be NP-hard, this
738 problem is rather abstract and from a practical perspective still too simplistic. For
739 a specific practical application the problem formulation needs to be tailored appro-
740 priately. Diverse aspects like different configuration options of stations, capacities or
741 time-dependent aspects may be needed to be considered. To a certain degree, the general
742 framework of COA can stay the same or may need only smaller adaptations, like for
743 example in the scenario generation of the FC.

744 Finally, we want to emphasize that the focus of this contribution was on the algorithmic
745 and computational aspects of COA and its components. Clearly, further challenges
746 concern a suitable user interface and a corresponding distributed implementation of at
747 least the FC, in which also psychological aspects of users need to be considered. More-
748 over, the performed experiments are based on the assumption of perfect user feedback,
749 which does not hold in practice. The impacts of not entirely reliable evaluation results
750 need to be studied, and robust variants of certain components of COA devised.

751 **Author Contributions:** Conceptualization, T.R.; methodology, T.R., G.R. and T.J.; software, valida-
752 tion, T.J.; writing—original draft preparation, T.J. and G.R.; writing—review and editing, T.J., G.R.
753 and T.R.; supervision, G.R. and T.R.; All authors have read and agreed to the published version of
754 the manuscript.

755 **Funding:** Thomas Jatschka was financially supported by the Honda Research Institute Europe.

756 **Institutional Review Board Statement:** Not applicable.

757 **Informed Consent Statement:** Not applicable.

758 **Data Availability Statement:** All of our benchmark instances are available online at <https://www.ac.tuwien.ac.at/research/problem-instances/#spd>. One instance group was derived
759 from the 2016 Yellow Taxi Trip Dataset: [https://data.cityofnewyork.us/Transportation/2016-
760 -Yellow-Taxi-Trip-Data/k67s-dv2t](https://data.cityofnewyork.us/Transportation/2016-Yellow-Taxi-Trip-Data/k67s-dv2t).

762 **Conflicts of Interest:** The authors declare no conflict of interest.

References

1. Gavalas, D.; Konstantopoulos, C.; Pantziou, G. Design and Management of Vehicle-Sharing Systems: A Survey of Algorithmic Approaches. In *Smart Cities and Homes*; Obaidat, M.S.; Nicopolitidi, P., Eds.; Elsevier, 2016; pp. 261–289.
2. Kloimüller, C.; Raidl, G.R. Hierarchical Clustering and Multilevel Refinement for the Bike-Sharing Station Planning Problem. International Conference on Learning and Intelligent Optimization. Springer, 2017, Vol. 10556, LNCS, pp. 150–165.
3. Xu, Y.; Shaw, S.L.; Fang, Z.; Yin, L. Estimating Potential Demand of Bicycle Trips from Mobile Phone Data—An Anchor-Point Based Approach. *ISPRS International Journal of Geo-Information* **2016**, *5*. doi:10.3390/ijgi5080131.
4. Wang, C.; Bi, J.; Sai, Q.; Yuan, Z. Analysis and Prediction of Carsharing Demand Based on Data Mining Methods. *Algorithms* **2021**, *14*. doi:10.3390/a14060179.
5. Schmidt, M.; Zmuda-Trzebiatowski, P.; Kiciński, M.; Sawicki, P.; Lasak, K. Multiple-Criteria-Based Electric Vehicle Charging Infrastructure Design Problem. *Energies* **2021**, *14*. doi:10.3390/en14113214.
6. Almaghrebi, A.; Aljuheshi, F.; Rifaie, M.; James, K.; Alahmad, M. Data-Driven Charging Demand Prediction at Public Charging Stations Using Supervised Machine Learning Regression Methods. *Energies* **2020**, *13*. doi:10.3390/en13164231.
7. Awasthi, A.; Venkitesamy, K.; Padmanaban, S.; Selvamuthukumar, R.; Blaabjerg, F.; Singh, A.K. Optimal planning of electric vehicle charging station at the distribution system using hybrid optimization algorithm. *Energy* **2017**, *133*, 70–78.
8. Cavadas, J.; Homem, G.d.A.C.; Gouveia, J. A MIP Model for Locating Slow-Charging Stations For Electric Vehicles in Urban Areas Accounting for Driver Tours. *Transportation Research Part E: Logistics and Transportation Review* **2015**, *75*, 188–201.

9. Dong, J.; Liu, C.; Lin, Z. Charging infrastructure planning for promoting battery electric vehicles: An activity-based approach using multiday travel data. *Transportation Research Part C: Emerging Technologies* **2014**, *38*, 44–55.
10. Pagany, R.; Camargo, L.R.; Dorner, W. A review of spatial localization methodologies for the electric vehicle charging infrastructure. *International Journal of Sustainable Transportation* **2019**, *13*, 433–449. doi:10.1080/15568318.2018.1481243.
11. Molin, E.; Mokhtarian, P.; Kroesen, M. Multimodal travel groups and attitudes: A latent class cluster analysis of Dutch travelers. *Transportation Research Part A: Policy and Practice* **2016**, *83*, 14–29. doi:https://doi.org/10.1016/j.tra.2015.11.001.
12. Radzimski, A.; Dziecielski, M. Exploring the relationship between bike-sharing and public transport in Poznań, Poland. *Transportation Research Part A: Policy and Practice* **2021**, *145*, 189–202.
13. Jatschka, T.; Rodemann, T.; Raidl, G.R. A Cooperative Optimization Approach for Distributing Service Points in Mobility Applications. *Evolutionary Computation in Combinatorial Optimization*; Liefoghe, A.; Paquete, L., Eds. Springer, 2019, Vol. 11452, LNCS, pp. 1–16.
14. Meignan, D.; Knust, S.; Frayret, J.M.; Pesant, G.; Gaud, N. A Review and Taxonomy of Interactive Optimization Methods in Operations Research. *ACM Transactions on Interactive Intelligent Systems* **2015**, *5*, 17:1–17:43.
15. Belton, V.; Branke, J.; Eskelinen, P.; Greco, S.; Molina, J.; Ruiz, F.; Słowiński, R. Interactive Multiobjective Optimization from a Learning Perspective. In *Multiobjective Optimization: Interactive and Evolutionary Approaches*; Branke, J.; Deb, K.; Miettinen, K.; Słowiński, R., Eds.; Springer, 2008; pp. 405–433.
16. Jatschka, T.; Rodemann, T.; R. Raidl, G. Exploiting Similar Behavior of Users in a Cooperative Optimization Approach for Distributing Service Points in Mobility Applications. *Machine Learning, Optimization, and Data Science*; Nicosia, G.; others., Eds. Springer, 2019, Vol. 11943, LNCS, pp. 738–750.
17. Devooght, R.; Kourtellis, N.; Mantrach, A. Dynamic Matrix Factorization with Priors on Unknown Values. Proceedings of the 21th ACM SIGKDD International Conference on Knowledge Discovery and Data Mining. ACM, 2015, p. 189–198.
18. Laporte, G.; Nickel, S.; Saldanha-da Gama, F., Eds. *Location Science*; Springer, 2015.
19. Cornuéjols, G.; Nemhauser, G.L.; Wolsey, L.A. The Uncapacitated Facility Location Problem. In *Discrete Location Theory*; Mirchandani, P.B.; Francis, R.L., Eds.; Wiley, 1990; pp. 119–171.
20. Snyder, L.V. Facility location under uncertainty: a review. *IIE Transactions* **2006**, *38*, 547–564.
21. Albareda-Sambola, M.; Fernández, E.; da Gama, F.S. The facility location problem with Bernoulli demands. *Omega* **2011**, *39*, 335–345. doi:https://doi.org/10.1016/j.omega.2010.08.002.
22. Turkeš, R.; Sörensen, K.; Cuervo, D.P. A matheuristic for the stochastic facility location problem. *Journal of Heuristics* **2021**.
23. Farahani, R.Z.; Hekmatfar, M. *Facility Location: Concepts, Models, Algorithms and Case Studies*; Springer, 2009.
24. Chen, T.; Kockelman, K.M.; Khan, M. The Electric Vehicle Charging Station Location Problem: A Parking-Based Assignment Method for Seattle. 92nd Annual Meeting of the Transportation Research Board in Washington DC, 2013.
25. Kameda, H.; Mukai, N. Optimization of Charging Station Placement by Using Taxi Probe Data for On-Demand Electrical Bus System. *Knowledge-Based and Intelligent Information and Engineering Systems*; König, A.; others., Eds. Springer, 2011, pp. 606–615.
26. Boyacı, B.; Zografos, K.G.; Geroliminis, N. An optimization framework for the development of efficient one-way car-sharing systems. *European Journal of Operational Research* **2015**, *240*, 718 – 733.
27. Frade, I.; Ribeiro, A. Bike-sharing stations: A maximal covering location approach. *Transportation Research Part A: Policy and Practice* **2015**, *82*, 216 – 227.
28. Frade, I.; Ribeiro, A.; Gonçalves, G.; Antunes, A. Optimal Location of Charging Stations for Electric Vehicles in a Neighborhood in Lisbon, Portugal. *Transportation Research Record: Journal of the Transportation Research Board* **2011**, *2252*, 91–98.
29. Vogel, P.; Greiser, T.; Mattfeld, D.C. Understanding Bike-Sharing Systems using Data Mining: Exploring Activity Patterns. *Procedia - Social and Behavioral Sciences* **2011**, *20*, 514 – 523.
30. Zhou, X. Understanding Spatiotemporal Patterns of Biking Behavior by Analyzing Massive Bike Sharing Data in Chicago. *PLOS ONE* **2015**, *10*, 1–20.
31. Trentini, A.; Losacco, F. Analyzing Carsharing “Public” (Scraped) Data to Study Urban Traffic Patterns. *Procedia Environmental Sciences* **2017**, *37*, 594 – 603.
32. Ciari, F.; Schuessler, N.; Axhausen, K.W. Estimation of Carsharing Demand Using an Activity-Based Microsimulation Approach: Model Discussion and Some Results. *International Journal of Sustainable Transportation* **2013**, *7*, 70–84.
33. Horni, A.; Nagel, K.; Axhausen, K.W., Eds. *Multi-Agent Transport Simulation MATSim*; Ubiquity Press, 2016.
34. Correia, G.H.D.A.; Jorge, D.R.; Antunes, D.M. The Added Value of Accounting For Users’ Flexibility and Information on the Potential of a Station-Based One-Way Car-Sharing System: An Application in Lisbon, Portugal. *Journal of Intelligent Transportation Systems* **2014**, *18*, 299–308.
35. Llorà, X.; Sastry, K.; Goldberg, D.E.; Gupta, A.; Lakshmi, L. Combating User Fatigue in iGAs: Partial Ordering, Support Vector Machines, and Synthetic Fitness. Proceedings of the 7th Annual Conference on Genetic and Evolutionary Computation. ACM, 2005, pp. 1363–1370.
36. Sun, X.; Gong, D.; Jin, Y.; Chen, S. A New Surrogate-Assisted Interactive Genetic Algorithm With Weighted Semisupervised Learning. *IEEE Transactions on Cybernetics* **2013**, *43*, 685–698.

37. Sun, X.Y.; Gong, D.; Li, S. Classification and Regression-based Surrogate Model-assisted Interactive Genetic Algorithm with Individual's Fuzzy Fitness. Proceedings of the 11th Annual Conference on Genetic and Evolutionary Computation. ACM, 2009, pp. 907–914.
38. Koziel, S.; Ciaurri, D.E.; Leifsson, L. Surrogate-based Methods. Computational Optimization, Methods and Algorithms. Springer, 2011, Vol. 356, *Studies in Computational Intelligence*, pp. 33–59.
39. Bell, R.M.; Koren, Y.; Volinsky, C. Matrix Factorization Techniques for Recommender Systems. *Computer* **2009**, *42*, 30–37.
40. Ekstrand, M.D.; Riedl, J.T.; Konstan, J.A. Collaborative Filtering Recommender Systems. *Foundations and Trends in Human-Computer Interaction* **2011**, *4*, 81–173.
41. Shi, L.; Rasheed, K. ASAGA: An Adaptive Surrogate-assisted Genetic Algorithm. Proceedings of the 10th Annual Conference on Genetic and Evolutionary Computation; ACM: NY, USA, 2008; pp. 1049–1056.
42. Mladenović, N.; Hansen, P. Variable Neighborhood Search. *Computers & Operations Research* **1997**, *24*, 1097–1100.
43. Jatschka, T.; Rodemann, T.; Raidl, G.R. VNS and PBIG as Optimization Cores in a Cooperative Optimization Approach for Distributing Service Points. Computer Aided Systems Theory – EUROCAST 2019; Moreno-Díaz, R.; others., Eds. Springer, 2020, Vol. 12013, *LNCS*, pp. 255–262.
44. Bouamama, S.; Blum, C.; Boukerram, A. A Population-based Iterated Greedy Algorithm for the Minimum Weight Vertex Cover Problem. *Applied Soft Computing* **2012**, *12*, 1632–1639.
45. Church, R.; ReVelle, C. The maximal covering location problem. *Papers in Regional Science*. Springer, 1974, Vol. 32, pp. 101–118.
46. Farahani, R.Z.; Asgari, N.; Heidari, N.; Hosseini, M.; Goh, M. Covering problems in facility location: A review. *Computers & Industrial Engineering* **2012**, *62*, 368 – 407.
47. Richtárik, P.; Takáč, M. Iteration complexity of randomized block-coordinate descent methods for minimizing a composite function. *Mathematical Programming* **2014**, *144*, 1–38.